

1 **Supplementary Material**

2 **Materials and Methods**

3 **Echocardiography**

4 Prior to initiation of the study, the mice were trained on two separate occasions over 1–2 days. Under
5 electrocardiographic monitoring of heart rate (HR, bpm), the hearts were imaged in 2D long-axis views at the level
6 of the highest left ventricular (LV) diameter. LV end-diastolic (LVIDd, mm) and end-systolic (LVIDs, mm) internal
7 diameters, end-diastolic wall thickness of both interventricular septum (IVS, mm) and LV posterior wall (LVPW,
8 mm), LV ejection fraction (EF, %) and fractional shortening (FS, %) were measured using M-mode in the
9 parasternal long-axis view. Relative wall thickness (RWT), a measure of hypertrophy, was calculated as
10 $IVSd+LVPWd/LVID$ (1).

11

12 **Pressure-volume loops**

13 Briefly, mice were anesthetized and mechanically ventilated through tracheostomy with 6–7 μ L/g tidal volume and
14 130 breaths/min under isoflurane. Blood volume expansion (12.5% human albumin, 50– 100 μ L over 5 min) was
15 provided through a 30-gauge cannula via the right external jugular vein. The LV apex was exposed through an
16 incision between the seventh and eighth ribs, and a 1.4-Fr PV catheter (SPR 839; Millar Instruments Inc.) was
17 advanced through the apex to lie along the longitudinal axis. Absolute left ventricular volume was calibrated, and
18 PV data were measured at steady state and during transient reduction of venous return by occluding the inferior vena
19 cava with a 6-0 silk snare suture. From the 10–15 successive cardiac cycles during the inferior vena cava occlusion,
20 the end-systolic PV relation slope was derived.)

21

22 **Electron paramagnetic resonance**

23 Briefly, ~20 mg of tissue was homogenized in phosphatebuffered saline (PBS) containing 0.1 mM diethylene-
24 triaminepentaacetic acid (DTPA) and protease inhibitor cocktail (Roche Applied Science, Indianapolis, IN) at pH
25 7.4. Nonsoluble fractions were removed by centrifugation at 15,000 g for 10 min at 4 oC. The homogenates were

26 kept on ice and analyzed immediately. Stock solutions of 1- hydroxy-3-methoxycarbonyl-2,2,5,5-
27 tetramethylpyrrolidine hydrochloride (CMH; Enzo Life Sciences, Farmingdale, NY) were prepared daily in nitrogen
28 purged 0.9% (w/v) NaCl, 25 g/L Chelex 100 (Bio-Rad) and 0.1 mM DTPA and kept on ice. The samples were
29 treated with 1 mM CMH at 37 oC for 2 min, transferred to 50- μ l glass capillary tubes, and analyzed on a Bruker E-
30 Scan (Billerica, MA) electron paramagnetic resonance (EPR) spectrometer at room temperature. EPR signal
31 intensities were normalized with respect to the protein concentrations of the tissue homogenates as determined by
32 Pierce BCA protein assay kit (Life Technologies).

33

34 **Elevated plus maze**

35 The test equipment consists of a four arms labyrinth two of which protected by lateral barriers (closed arms, 30 cm \times
36 5 cm, \times 15 cm) and the other two exposed (open arms, 30 cm \times 5 cm, 350 lx). EPM exploits the rodent's conflict
37 between aversion to open spaces (i.e. hides in closed arms of a labyrinth) and instinct to explore new environments
38 (i.e. exploration of open arms of the same labyrinth). The experimental sessions have been videotaped by camera
39 placed above the apparatus.)

40 **Y-maze**

41 (The test equipment consists of a Y-shaped labyrinth composed of three arms (30 cm \times 5 cm \times 15 cm). Y-maze test
42 is based on the tendency of the mouse to explore new environments, hence preferring a labyrinth arm not yet
43 explored to an already known one (2). The experimental sessions have been videotaped by camera placed above the
44 apparatus.)

45

46 **Histological analyses**

47 All antibodies are listed in Supplementary Table 1.

48 **Heart**

49 Slides were obtained from FFPE blocks (5 μ m thick), then were deparaffinized with xylene, rehydrated with three
50 consecutive ethanol washes (100%, 75%, and 30%) and two 1X PBS washes, underwent antigen retrieval (10mM

51 Tris 1mM EDTA, 10mins in pressure cooked), and blocked (5% BSA, 0.1% Triton-X, 1X PBS) for 1 hour at room
52 temperature. Deparaffinized tissue sections were stained with antibodies shown in Supplementary Table 1. First,
53 myocardium was incubated overnight at 4°C with mouse monoclonal antibody against cardiac troponin T (1:250;
54 Thermo Fisher Scientific, Cat. No. MA5-12960). The following day, slides were washed three times with 1X PBS
55 and then incubated with donkey anti-mouse Alexa Fluor 555 (1:250, Abcam, Cat.No. ab150106) for one hour at
56 room temperature. Following three 1X PBS washes, slides underwent TUNEL staining using an in situ cell death
57 detection kit according to manufacturer's protocol (Roche Applied Science, 12156792910). Following TUNEL
58 staining, slides were washed three times with 1X PBS, then Fluoroshield with DAPI (Sigma, Cat. No. F6057) was
59 added to slides and cover slipped. Immunoreactive signal was detected via laser scanning microscopy (Zeiss LSM
60 510 Meta). Sections were imaged on an Olympus BX51TF with a DP70 color camera (Olympus). Collagen was
61 quantified in digitally acquired images (3). CSA was computed on cardiomyocytes in perfect transverse section
62 with a centrally localized nucleus. To compute cardiomyocyte nuclear densities, 15-20 images per animal at 630X
63 magnification were acquired and analyzed.

64 **Hippocampus**

65 Sections were cut in anteroposterior direction using a freezing microtome (Leica, Germany). Serial sections (one out
66 of six) were selected to perform immunohistochemical staining of Parvalbumin (1:200, Synaptic System, Germany)
67 and Glial fibrillary acidic protein (1:500 GFAP, Agilent, USA). Signal was revealed with 2 h incubation with,
68 respectively, anti-guinea pig Alexa488 (1:500, Jackson ImmunoResearch) and anti-rabbit Rhodamine Red X (1:500,
69 Jackson ImmunoResearch). For BrdU detection, free-floating sections were pretreated by denaturing DNA with 2 M
70 HCl for 30 min at 37 °C . Slices were blocked for 1 h at room temperature (RT) with 10% normal goat serum
71 (NGS), 0.3% Triton X-100 in PBS, and then incubated overnight at 4 °C with a rat monoclonal anti-BrdU antibody
72 (1:200, Abcam, AB6326) diluted in NGS 5% and Triton 0.1% in PBS. Signal was finally revealed with 2 h
73 incubation at RT with Cy3 conjugated anti-rat IgG (1:500, Jackson Immuno Research). We also performed a double
74 labeling for BrdU and neuronal nuclei (NeuN, 1:1000, Millipore, revealed with AlexaFluor488 anti-guinea pig IgG
75 (1:400, Jackson Immuno Research). Cells were counted on a fluorescence microscope (Zeiss) using a 20 × objective
76 and the analysis was performed using Stereo Investigator software (Microbrightfield). All cells in the granule cell
77 layer and subgranular zone of every sixth section were counted, and the resulting number of cells was multiplied by

78 6 to give an estimate of the total number of labeled cells. The quantification of GFAP expression was performed
79 offline on images captured with a microscope (Axio Imager. Z2, Zeiss) equipped with Apotome.2 (Zeiss) with a 20
80 × EC-PLAN-NEOFLUAR objective. Z-series stacks were acquired with an interval of 1 μm for 3 slices per animal.
81 Maximum intensity projections were produced and the analysis was performed using Fiji (ImageJ software). Images
82 were first converted to 8 bit and 3 200 μm wide ROIs of DG, CA1 and CA2/3 were selected. For the 3 ROIs the
83 mean grey value was calculated and normalized using the value taken from the same ROI in a control image
84 acquired in the thalamus of the same slice where only background labeling was present. Normalized values of the 3
85 ROIs of the single animal were then averaged to obtain the mean GFAP expression value of the single animal. The
86 total amount of GFAP staining was then given as the mean ±standard error for each experimental group.

87

88

89 **References**

90

91 1. Sebag IA, Gillis MA, Calderone A, Kasneci A, Meilleur M, Haddad R, et al. Sex hormone control of left
92 ventricular structure/function: mechanistic insights using echocardiography, expression, and DNA methylation
93 analyses in adult mice. *Am J Physiol Heart Circ Physiol.* 2011;301(4):H1706-15.

94 2. Maynard KR, Hill JL, Calcaterra NE, Palko ME, Kardian A, Paredes D, et al. Functional Role of BDNF
95 Production from Unique Promoters in Aggression and Serotonin Signaling. *Neuropsychopharmacology.*
96 2016;41(8):1943-55.

97 3. Lionetti V, Matteucci M, Ribezzo M, Di Silvestre D, Brambilla F, Agostini S, et al. Regional mapping of
98 myocardial hibernation phenotype in idiopathic end-stage dilated cardiomyopathy. *J Cell Mol Med.* 2014;18(3):396-
99 414.

100

101

102

103 **Supplementary Tables**104 **Supplementary Table 1.**

Antigen	Antibody (species)	Company	Antigen retrieval	Dilution	Incubation time and temperature	Secondary Antibody (fluorochrome and dilution)	Incubation time and temperature
Alpha-Sarcomeric Actin	Mouse monoclonal	Sigma #A2172	Citric buffer (pH6), 98°C, 40'	1:400	1h, 37°C	Cy5 1:400	1h, 37°C
Cardiac Troponin T	Mouse monoclonal	Thermo Fisher Scientific #MA5-12960	Citric buffer (pH6), 98°C, 40'	1:250	1h, 37°C	Alexa555 1:250	1h, 37°C
Glial fibrillary acidic protein (GFAP)	Rabbit polyclonal	DAKO #Z0334		1:500	O/N, 4°C	RRX 1:500	2h, RT
Parvalbumin	Guinea Pig polyclonal	Synaptic System, Germany #195 004		1:300	1h, 37°C	Alexa488 1:500	2h, RT
Smooth Muscular Actin	Mouse monoclonal	DAKO #M0851	Citric buffer (pH6), 98°C, 40'	1:100	O/N, 4°C	Alexa488 1:600	1h, 37°C
Isolectin GS-IB4 Biotin conjugated	Molecular probe	Thermo Fisher Scientific #121414	Citric buffer (pH6), 98°C, 40'	1:200	O/N, 4°C	Streptavidin DyLight550 (Abcam ab 134348)1:200	1h, 37°C
Hoechst 33258		Thermo Fisher Scientific Cat# H3569		1:1000	3 min, RT		

Anti-BrDU	Rat polyclonal	AbCAM, ab152095	HCl 2MOL, 37°C, 30'	1:500	O/N, 4°C	CY3 1:500	2h, RT
Anti-NeuN	Guinea Pig polyclonal	MILLIPO RE ABN90		1:1000	O/N, 4°C	Alexa488 1:400	2h, RT

105

106

107

108

109

110

111

112

113

114

115

116

117

118

119

120 **Supplementary Figure Legends**

121 **Suppl. Figure 1.** Representative scheme of resident intruder paradigm. (a) Resident CD1 mouse. (b) 10 minutes
122 interaction among resident CD1 and intruder C57BL/6J mouse. (c) Resident and intruder separated by a perforated
123 partition, which maintains them in continuous sensory contact.

124 **Suppl. Figure 2.** Number of attacks in mice fed with standard diet (Control) or high fat diet (HFD).

125 **Suppl. Figure 3.** PS in obese mice increases apoptosis of left ventricular (LV) cardiac cells. (a) Representative
126 images of the detection of LV apoptotic cardiac cells in each experimental group after staining with cardiac
127 troponin T.DAPI, 4',6-diamidino-2-phenylindole; TUNEL, terminal deoxynucleotidyltransferase/UTP nick end
128 labeling. (b) LV fraction of cardiac troponin positive cells that are TUNEL positive (%). All values are represented
129 through box-and-whisker plots (n=4-5 per group, two-way ANOVA, **p < 0.01 Vs Controls; # p<0.05 Vs Ob;
130 \$\$p<0.01 Vs PS; &p<0.05 interaction between Ob and PS).

131 **Suppl. Figure 4.** Obesity and PS doesn't affect number of PV+ cells and volume of CA1 and CA2/3 regions but
132 target an increased inflammatory state in all the hippocampal structures. Average measure of CA1 (a) and CA2/3 (b)
133 volume quantified with Hoechst staining. Relative expression of GFAP in CA1 (c) and CA2/3 (d) hippocampal
134 regions. Average number of PV+ interneurons in CA1 (e) and CA2/3 (f) regions. All values are represented through
135 box-and-whisker plots (n=4-5 per group, two-way ANOVA, **p < 0.01 and ***p < 0.001 Vs Controls; # p<0.05
136 and ## p < 0.01 Vs Ob; \$\$ p<0.01 Vs PS; &p<0.05 interaction between Ob and PS).

137 **Suppl. Figure 5.** Western blots assay of hippocampal tissues. Panel (a) and (b) show the full-length Western blots
138 corresponding to cropped blots in the main text.

139

140

141

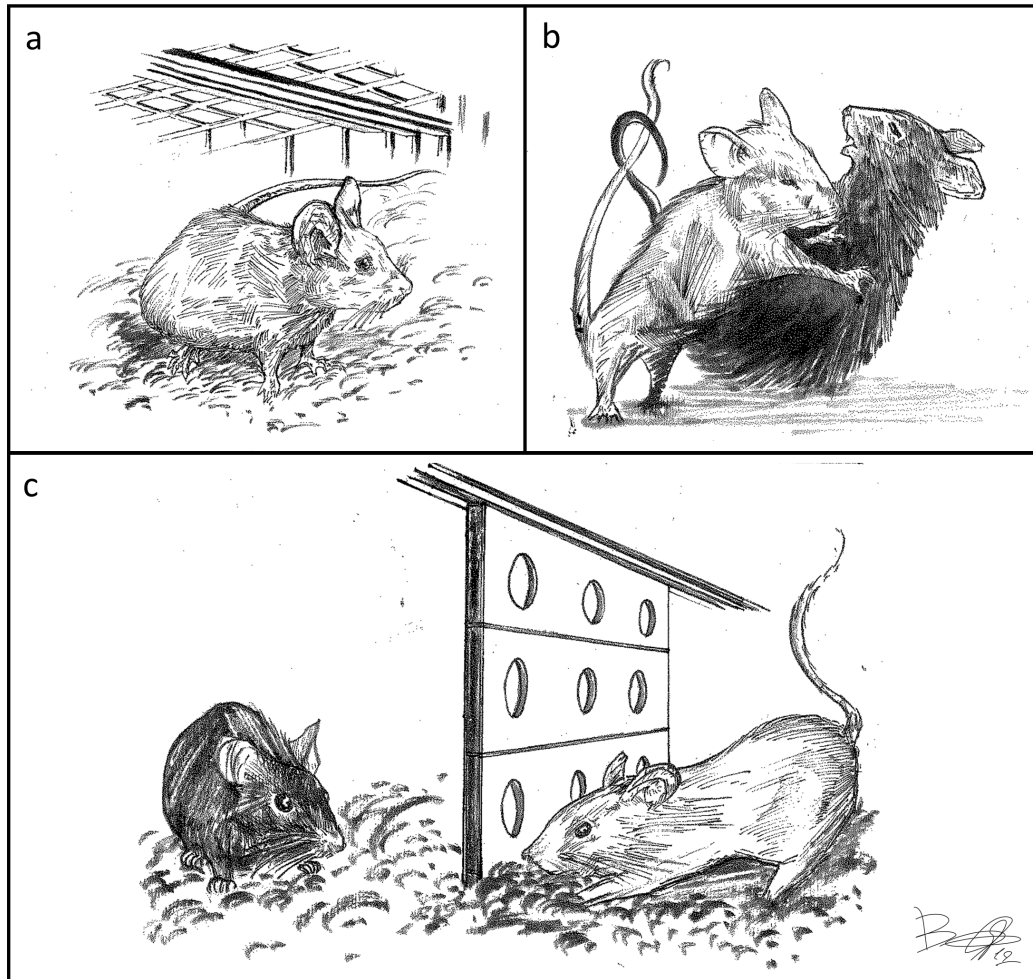
142

143

144

145

146 **Suppl. Figure 1.**



147

148

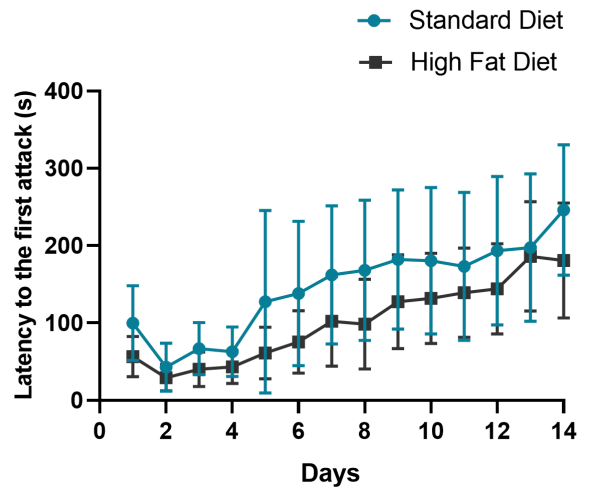
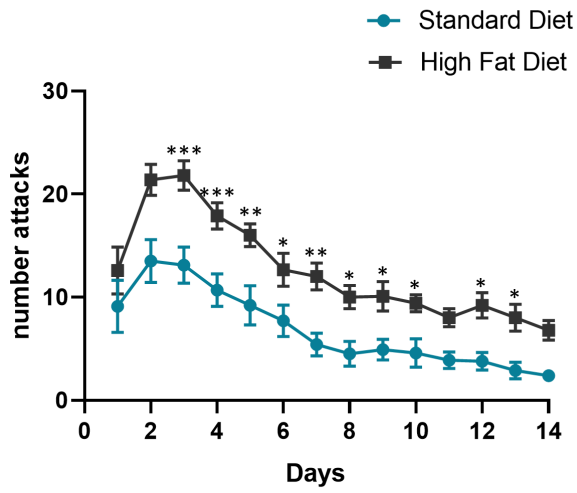
149

150

151

152

153 **Suppl. Figure 2.**



154

155

156

157

158

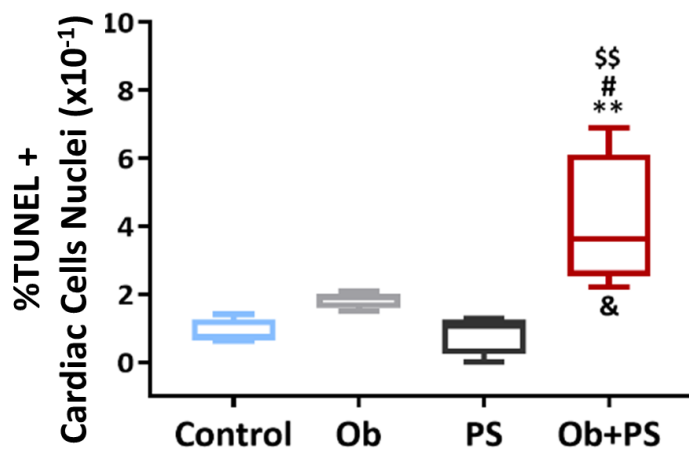
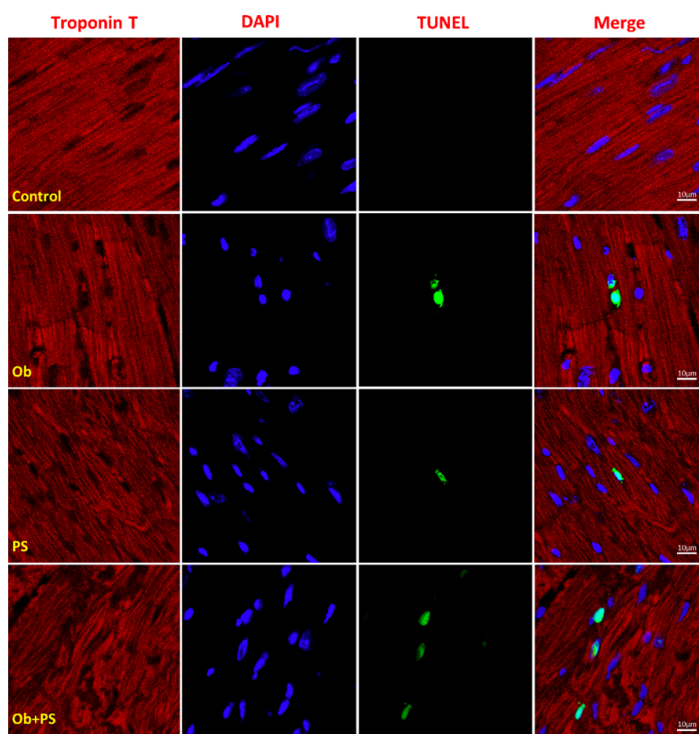
159

160

161

162

163 **Suppl. Figure 3.**

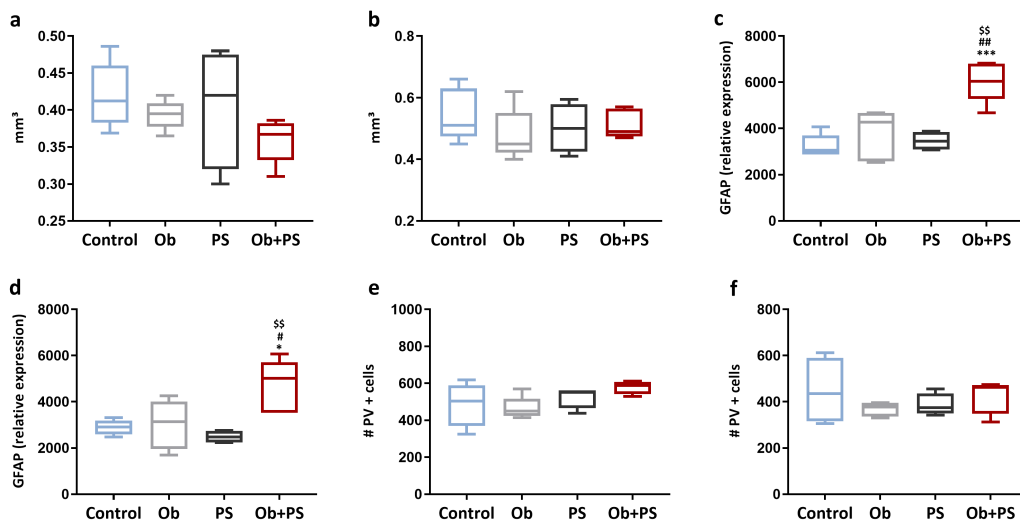


164

165

166
167
168
169
170
171
172
173
174
175
176

Suppl. Figure 4.



177
178
179
180
181
182
183
184

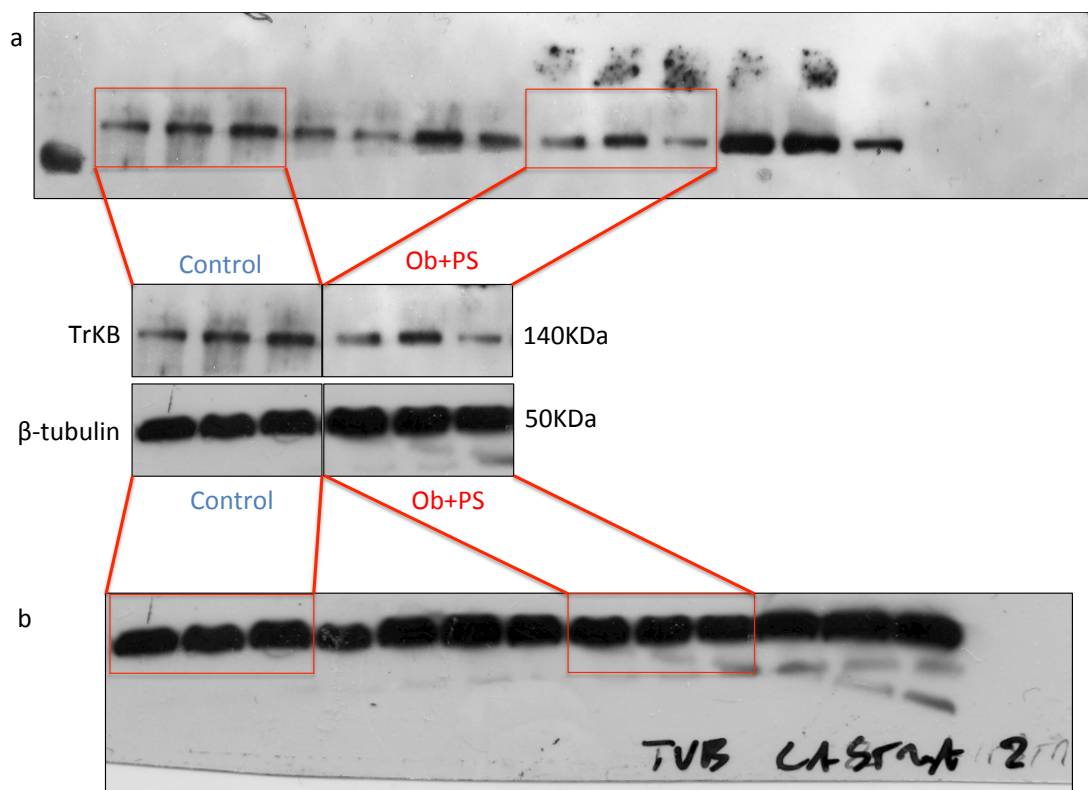
185 **Suppl. Figure 5.**

186

187

188

189



190